J. Appl. Comput. Mech., 7(2) (2021) 913-921
DOI: 10.22055/JACM.2021.36043.2783

ISSN: 2383-4536
jacm.scu.ac.ir

Shahid Chamran University of Ahvaz

Journal of Applied and Computational Mechanics

Research Paper

Nonlinear Dynamic Behavior of Hyperbolic Paraboloidal Shells Reinforced by Carbon Nanotubes with Various Distributions

Elcin Yusufoglu[1], Mahmure Avey[2]

[1] Department of Mathematics, Faculty of Arts and Sciences, Usak University, 64200 Usak, Turkey

[2] Division of Mathematics, Graduate School of Natural and Applied Sciences, Usak University, 64200 Usak, Turkey

Received December 12 2020; Revised January 08 2021; Accepted for publication January 09 2021.
Corresponding author: M. AVEY (mahmureavey@gmail.com)

Abstract. The analytical solution of the nonlinear dynamic behavior of CNT-based hyperbolic paraboloidal shallow shells (HYPARSSs) with various distribution shapes is presented. A theoretical model was created for HYPARSSs reinforced with CNTs using the von Kármán -type nonlinearity. Then the nonlinear basic equations are reduced to ordinary nonlinear differential equations using Galerkin methods and the correlation for frequency-amplitude relationship is obtained using the Grigolyuk method. In addition, the nonlinear frequency/linear frequency (NL/L) ratio is determined as a function of amplitude. Comparisons with reliable results in the literature were made to test the accuracy of the formulas. Finally, a systematic investigate is performed to control the influences of CNTs in the matrix, CNT distribution types and nonlinearity on the vibration frequency-amplitude relationship.

Keywords: Nonlinear dynamics, CNTs, Hyperbolic paraboloidal shallow shells, Amplitude-frequency relationship.

1. Introduction

The hyperbolic paraboloidal shells are doubly curved shells with negative Gaussian curvature; they are called HP or HYPAR shells, and a subclass of them is called saddle-type shells. Based primarily on their effectiveness, these geometric structural forms are used in a number of industrial applications such as pressure vessels, protective structures, etc. [1-4]. Considering the practical importance of nonlinear vibrations (NLVs) of double-curved composite shallow shells, many researchers have carried out research on this topic [5-10].

Advances in material technology have made it possible to produce new nano- composite materials reinforced with carbon nanotubes to meet the demand for more efficient and lighter vehicles. The widespread use of nanotechnology in many practical areas began with the discovery of carbon nanotubes (CNTs) by Iijima in 1991 [11]. The production of aligned carbon nanotubes has led to the use of composites reinforced by CNTs in various engineering disciplines [12]. Basic knowledge about the features of CNTs, potential and current challenges are contained in the work of refs. [13-17]. There are fundamental studies in the literature on the determination of material properties and production method of composites reinforced by CNTs [18, 19].

At present, researchers are more interested in the nonlinear vibrational behavior of heterogeneous composite shells reinforced by CNTs, realizing the potential of modern applications for new generation heterogeneous materials due to the outstanding properties of CNTs. The first attempt to solve the nonlinear vibration problems of heterogenous shells reinforced by CNT (generally cylindrical shells) was made by Shen and colleagues [20, 21]. In the above studies, theoretical modeling of functionally graded (FG)-CNTRC cylindrical shells was carried out and opportunities were provided to formulate various vibration and stability problems. Based on this scientific basis, various vibration problems of CNT-based composite shells were solved using analytical and finite element methods in linear and nonlinear settings [22-37].

The behavior of thin-walled HYPAR shallow shells (HYPARSSs) reinforced by functionally graded CNTs, taking into account geometric nonlinearity, has not been sufficiently studied, which is associated with the complexity of the configuration type, as well as the difficulties arising in solving nonlinear problems. Therefore, the development of a mathematical model of the deformation of HYPARSSs taking into account the above factors (heterogeneity and nonlinearity) and the study of the behavior of such shells in a nonlinear formulation is an urgent task. The aim of this work is to solve the NL dynamic problem of HYPARSSs reinforced by CNTs, using superposition, Galerkin and Grigolyuk methods, as well as to establish a relationship between nonlinear frequency and amplitude.

2. Formulation of the problem

The HYPARSS reinforced by CNTs with the thickness h, the length a, the width b, and the mean radii of curvature R_1 and R_2, respectively, is shown in Fig. 1. The orthogonal coordinate system (x,y,z) is located on the reference surface. The displacement components u, v and w of the hyperbolic paraboloidal shell are in the x, y and z directions, respectively.

Published online: January 10 2021

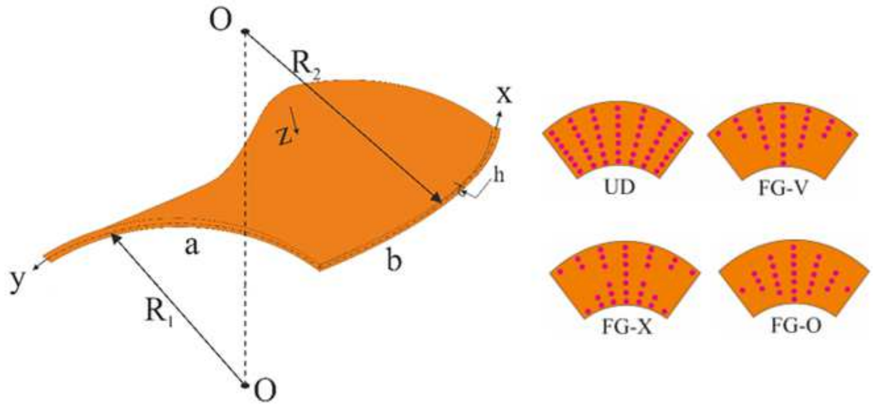

(a) (b)

Fig. 1. (a) Hyperbolic paraboloidal shallow shell and coordinate system (b) four types of CNT distributions

The materials of HYPARSSs have been developed to four distributions of CNTs along the thickness direction, including a uniformly distributed (UD) and three types of linear function (FG-V, FG-O, FG-X) as follows (see, Fig. 1b) [20]:

$$V_{cn}^{z_1}=\begin{cases} UD \quad for \quad V_{cn}^{*} \\ FG-V \quad for \quad (1-2z_1)V_{cn}^{*} \\ FG-O \quad for \quad (1+2z_1)V_{cn}^{*} \\ FG-X \quad for \quad 4|z_1|V_{cn}^{*} \end{cases} \tag{1}$$

Here $z_1 = zh^{-1}$ is dimensionless thickness coordinate, V_{cn}^{*} is total volume fraction of CNTs and determined by

$$V_{cn}^{*}=\frac{w_{cn}}{w_{cn}+(\rho_{cn}/\rho_m)(1-w_{cn})} \tag{2}$$

in which w_{cnt} is the CNT mass fraction, ρ_{cnt} and ρ_m are the mass densities of CNT and matrix, respectively. It can be seen from the volume fractions of CNTs that the total mass fractions of CNTs in the HYPARSSs with FG-V, FG-O, FG-X and UD types are the same.

2.1. Material Properties

The effective material properties of the two-phase composites, mixture of CNTs and in isotropic matrix, and are predicted by the extended rule of mixture [21, 22]:

$$\begin{aligned} &E_{11}^{z_1}=\eta_1 V_{cn}^{z_1}E_{11}^{cn}+V_m E_m,\; E_{22}^{z_1}=\frac{\eta_2 E_m E_{22}^{cn}}{E_{22}^{cn}V_m+E_m V_{cn}^{z_1}},\; G_{12}^{z_1}=\frac{\eta_3 G_m G_{12}^{cn}}{G_{12}^{cn}V_m+G_m V_{cn}^{z_1}} \\ &\nu_{12}=V_{cn}^{*}\nu_{12}^{cn}+V_m\nu_m,\; \rho_1^{z_1}=V_{cn}^{z_1}\rho_{cn}+V_m\rho_m \end{aligned} \tag{3}$$

where E_m, G_m, ρ_m, ν_m and $E_{ij}^{cn}, G_{ij}^{cn}, \rho_{cn}, \nu_{12}^{cn}$ $(i,j=1,2)$ denote the symbols for Young's modulus, shear modulus, density and Poisson's ratio for the matrix and properties of CNT phase, respectively, $\eta_i(i=1,2,3)$ denotes CNT/matrix efficiency parameters, that defines scale-dependent material properties. V^m is the matrix volume fraction that obey the rule of $V_{cnt}^{\bar{z}}+V_m=1$.

2.2. Constitutive relations and basic equations

The basic relations of HYPARSSs reinforced with carbon nanotubes, based on the Kirchhoff-Love hypothesis, can be constructed as follows [20, 32]:

$$\begin{bmatrix}\sigma_{11}\\ \sigma_{22}\\ \sigma_{12}\end{bmatrix}=\begin{bmatrix}\frac{E_{11}^{z_1}}{1-\nu_{12}\nu_{21}} & \frac{E_{12}^{z_1}}{1-\nu_{12}\nu_{21}} & 0\\ \frac{E_{21}^{z_1}}{1-\nu_{12}\nu_{21}} & \frac{E_{22}^{z_1}}{1-\nu_{12}\nu_{21}} & 0\\ 0 & 0 & G_{12}^{z_1}\end{bmatrix}\begin{bmatrix}\varepsilon_{11}\\ \varepsilon_{22}\\ \varepsilon_{12}\end{bmatrix} \tag{4}$$

In the relation (4), σ_{ij} and $\varepsilon_{ij}(i,j=1,2)$ denote the symbols for stresses and strains of HYPARSSs reinforced by carbon nanotubes and the forces $N_{ij}(i,j=1,2)$ and moments $M_{ij}(i,j=1,2)$ are defined as [38]:

$$\left(N_{ij},M_{ij}\right)=\int_{-h/2}^{h/2}\left(\sigma_{ij},z\sigma_{ij}\right)dz, \tag{5}$$

Airy stress function Ψ defines as [38]:

$$\left(N_{11},N_{22},N_{12}\right)=h\left(\Psi_{,yy},\,\Psi_{,xx},\,-\Psi_{,xy}\right) \tag{6}$$

where (,) denotes partial derivatives with respect to coordinates.

Substituting relations (4) into (5) and using relations (6), the following expressions for strains on the mid-surface and moments of CNT-based HYPARSSs with the independent parameters Ψ and w is obtained:

$$\begin{Bmatrix} \varepsilon_{11} \\ \varepsilon_{22} \\ \gamma_{12} \end{Bmatrix} = \begin{bmatrix} b_{11} & b_{12} & 0 \\ b_{21} & b_{22} & 0 \\ 0 & 0 & b_{31} \end{bmatrix} \begin{Bmatrix} \Psi_{,yy} \\ \Psi_{,xx} \\ -\Psi_{,xy} \end{Bmatrix} - \begin{bmatrix} b_{13} & b_{14} & 0 \\ b_{23} & b_{24} & 0 \\ 0 & 0 & b_{32} \end{bmatrix} \begin{bmatrix} w_{,xx} \\ w_{,yy} \\ w_{,xy} \end{bmatrix} \tag{7}$$

$$\begin{Bmatrix} M_{11} \\ M_{22} \\ M_{12} \end{Bmatrix} = \begin{bmatrix} c_{11} & c_{12} & 0 \\ c_{21} & c_{22} & 0 \\ 0 & 0 & c_{31} \end{bmatrix} \begin{Bmatrix} \Psi_{,yy} \\ \Psi_{,xx} \\ -\Psi_{,xy} \end{Bmatrix} - \begin{bmatrix} c_{13} & c_{14} & 0 \\ c_{23} & c_{24} & 0 \\ 0 & 0 & c_{32} \end{bmatrix} \begin{bmatrix} w_{,xx} \\ w_{,yy} \\ w_{,xy} \end{bmatrix} \tag{8}$$

The symbols in relations (7) and (8) are defined as follows:

$$\begin{aligned} & c_{11} = a_{11}^1 b_{11} + a_{12}^1 b_{21},\ c_{12} = a_{11}^1 b_{12} + a_{12}^1 b_{11},\ c_{13} = a_{11}^1 b_{13} + a_{12}^1 b_{23} + a_{11}^2,\ c_{14} = a_{11}^1 b_{14} + a_{12}^1 b_{24} + a_{12}^2, \\ & c_{21} = a_{21}^1 b_{11} + a_{22}^1 b_{21},\ c_{22} = a_{21}^1 b_{12} + a_{22}^1 b_{22},\ c_{23} = a_{21}^1 b_{13} + a_{22}^1 b_{23} + a_{21}^2,\ c_{24} = a_{21}^1 b_{14} + a_{22}^1 b_{24} + a_{22}^2, \\ & c_{31} = a_{66}^1 b_{35}, c_{32} = a_{66}^1 b_{32} + 2a_{66}^2, b_{11} = \frac{a_{22}^0}{\mu}, b_{12} = -\frac{a_{12}^0}{\mu}, b_{13} = \frac{a_{12}^0 a_{21}^1 - a_{11}^1 a_{22}^0}{\mu}, b_{14} = \frac{a_{12}^0 a_{22}^1 - a_{12}^1 a_{22}^0}{\mu}, \\ & b_{21} = -\frac{a_{21}^0}{\mu},\ b_{22} = \frac{a_{11}^0}{\mu},\ b_{23} = \frac{a_{11}^1 a_{21}^0 - a_{21}^1 a_{11}^0}{\mu},\ b_{24} = \frac{a_{12}^1 a_{21}^0 - a_{22}^1 a_{11}^0}{\mu},\ b_{31} = \frac{1}{a_{66}^0},\ b_{32} = -\frac{2a_{66}^1}{a_{66}^0} \end{aligned} \tag{9}$$

where

$$\begin{aligned} & \mu = a_{11}^0 a_{22}^0 - a_{12}^0 a_{21}^0,\ a_{11}^i = \frac{\int_{-h/2}^{h/2} E_{11}^{z_1} z^i dz}{1 - \nu_{12}\nu_{21}},\ a_{12}^i = \frac{\int_{-h/2}^{h/2} \nu_{21} E_{11}^{z_1} z^i dz}{1 - \nu_{12}\nu_{21}},\ a_{21}^k = \frac{\int_{-h/2}^{h/2} \nu_{12} E_{22}^{z_1} z^i dz}{1 - \nu_{12}\nu_{21}}, \\ & a_{22}^i = \frac{\int_{-h/2}^{h/2} E_{22}^{z_1} z^i dz}{1 - \nu_{12}\nu_{21}},\ a_{66}^i = \int_{-h/2}^{h/2} G_{12}^{z_1} z^i dz,\ i = 0,1,2. \end{aligned} \tag{10}$$

in which the strains on the reference surface of HYPARSSs reinforced by carbon nanotubes include the von Kármán-type nonlinear terms [38]:

$$\begin{bmatrix} \varepsilon_{11} \\ \varepsilon_{22} \\ \gamma_{12} \end{bmatrix} = \begin{bmatrix} u_{,x} - w / R_1 + 0.5 w_{,x}^2 \\ u_{,y} + w / R_2 + 0.5 w_{,y}^2 \\ v_{,x} + u_{,y} + w_{,x} w_{,y} \end{bmatrix} \tag{11}$$

Introducing (6)-(8) into the nonlinear motion and compatibility equations of shallow shells [38], the nonlinear basic equations of HYPARSSs reinforced by carbon nanotubes take the following form:

$$\begin{aligned} & h\left[c_{12}\ \Psi_{,xxxx} + (c_{11} - 2c_{31} + c_{22})\ \Psi_{,xxyy} + c_{21}\Psi_{,yyyy}\right] - c_{13}\ w_{,xxxx} - (c_{14} + 2c_{32} + c_{23})\ w_{,xxyy} - c_{24}\ w_{,yyyy} \\ & + h\left[\Psi_{,xx} / R_2 - \Psi_{,yy} / R_1 + \Psi_{,yy} w_{,xx} - 2\Psi_{,xy} w_{,xy} + \Psi_{,xx} w_{,yy}\right] = \rho_1 \ddot{w} \end{aligned} \tag{12}$$

$$\begin{aligned} & h\left[b_{11}\Psi_{,yyyy} + (b_{12} + b_{21} + b_{31})\Psi_{,xxyy} + b_{22}\Psi_{,xxxx}\right] - b_{23} w_{,xxxx} - (b_{24} + b_{13} - b_{32}) w_{,xxyy} \\ & - b_{14} w_{,yyyy} + w_{,xx} / R_2 - w_{,yy} / R_1 - w_{,xy}^2 + w_{,xx} w_{,yy} = 0 \end{aligned} \tag{13}$$

where $(\bullet)$ denotes partial derivatives with respect to time, the time parameter will be represented by τ, and the following definition applies:

$$\rho_1 = \rho_{cn} \int_{-h/2}^{h/2} V_{cn}^{z_1} dz + V_m \rho_m h \tag{14}$$

3. Solution procedure

The approximation function for the deflection of simply-supported CNT-based HYPARSSs is sought as [38, 39]:

$$w = \bar{w}(t)\sin(k_1 x)\sin(k_2 y) \tag{15}$$

where $k_1 = m\pi / a$, $k_2 = n\pi / b$, and $\bar{w}(\tau)$ is a time-dependent function.

Letting (15) in the Eq. (13), one gets

$$\Psi = u_1 \bar{w}^2 \cos(2k_1 x) + u_2 \bar{w}^2 \cos(2k_2 y) + u_3 \bar{w} \sin(k_1 x)\sin(k_2 y) \tag{16}$$

where

$$u_1 = \frac{k_2^{\,2}}{32k_1^{\,2}b_{22}h},\; u_2 = \frac{k_1^{\,2}}{32k_2^{\,2}b_{11}h},\; u_3 = \frac{b_{23}k_1^{\,4} + (b_{24} + b_{13} - b_{32})k_1^{\,2}k_2^{\,2} + b_{14}k_2^{\,4} + k_1^{\,2}/R_2 - k_2^{\,2}/R_1}{h\left[b_{11}k_2^{\,4} + (b_{12} + b_{21} + b_{31})k_1^{\,2}k_2^{\,2}\right] + b_{22}k_1^{\,4}} \tag{17}$$

Substituting (15) and (16) into Eq. (12), and using Galerkin method, one gets

$$\ddot{\bar{w}}(\tau) + \omega_L^2\bar{w}(\tau) + \Gamma_1\bar{w}^2(\tau) + \Gamma_2\bar{w}^3(\tau) = 0 \tag{18}$$

where ω_L denotes natural or linear frequency of HYPARSSs reinforced by carbon nanotubes and expressed as:

$$\omega_L^2 = \left\{\left[-k_2^2/R_1 + k_1^2/R_2 - c_{12}k_1^{\,4} - (c_{11} - 2c_{31} + c_{22})k_1^{\,2}k_2^{\,2} - c_{21}k_2^{\,4}\right]hu_3 + c_{13}k_1^{\,4} + (c_{14} + 2c_{32} + c_{24})k_1^{\,2}k_2^{\,2} + c_{24}k_2^{\,4}\right\}/\rho_1 \tag{19}$$

and

$$\begin{aligned}\Gamma_1 &= 64h\left[c_{12}k_1^{\,3}u_1/k_2 + c_{21}k_2^{\,3}u_2/k_1 - 0.125k_1k_2u_3 + 0.25u_1k_1/(R_2k_2) - 0.25u_2k_2/(R_1k_1)\right]\times\left[1-(-1)^m-(-1)^n+(-1)^{m+n}\right]/(3\rho_1 ab)\\ \Gamma_2 &= 2hk_1^{\,2}k_2^{\,2}(u_1+u_2)/\rho_1\end{aligned} \tag{20}$$

Introducing (21) into (18), after some operations, an equation of the type $L(\tau)=0$ is obtained. To determine the amplitude-frequency dependence of the NLV for HYPARSS reinforced with carbon nanotubes, the method proposed by Grigolyuk [39] is used for the above obtained equation, which satisfies the orthogonality condition:

$$\int_0^{\pi/2} L(\tau)\cos(\omega_{NL}\tau)\,d\tau = 0 \tag{21}$$

where ω_{NL} is the frequency of the NLV for HYPARSSs reinforced by carbon nanotubes.

The approximate function is expressed as follows:

$$\bar{w}(\tau) = w_0\cos(\omega_{NL}\tau) \tag{22}$$

where w_0 is the amplitude and the initial conditions are described as:

$$\bar{w}(\tau)\Big|_{\tau=0} = w_0 \;\text{ and }\; \frac{d\bar{w}(\tau)}{d\tau}\Big|_{\tau=0} = 0 \tag{23}$$

Integrating the Eq. (21) taking into account (22), we obtain:

$$\omega_{NL} = \left(\omega_L^2 + \frac{8}{3\pi}\Gamma_1 fh + \frac{3}{4}\Gamma_2 h^2 f^2\right)^{1/2} \tag{24}$$

where $f = w_0/h$ denotes a non-dimensional amplitude parameter.

The Eq. (24) describes the amplitude-frequency relationship of the NLV for HYPARSSs reinforced by carbon nanotubes.

The nonlinear frequency to linear frequency ratio (ω_{NL}/ω_L) of HYPARSSs reinforced by carbon nanotubes is determined as:

$$\omega_{NL}/\omega_L = \left(1 + \frac{8}{3\pi}\frac{\Gamma_1 fh}{\omega_L^{\,2}} + \frac{3}{4}\frac{\Gamma_2 h^2 f^2}{\omega_L^{\,2}}\right)^{1/2} \tag{25}$$

The minimum magnitudes of ω_{NL} and ω_{NL}/ω_L for HYPARSSs reinforced by carbon nanotubes are obtained by minimizing Eqs. (24) and (25) depending on the vibration modes for fixed values of f.

4. Numerical Results

4.1. Material properties of CNTs and matrix

In this subsection, the material point of view, polymethyl methacrylate (PMMA) is selected as the matrix with the material properties: $E_m = 0.25\times10^{10}$Pa, $\nu_m = 0.34$, $\rho_m = 1.15\times10^3$kg/m^3 . In addition, single-walled carbon nanotubes (SWCNTs) as reinforcement with (10, 10) armchair structure with the material properties: $\bar{r} = 9.26$nm, $\bar{a} = 0.68$nm, $\bar{h} = 0.067$nm , and $E_{11}^{cn} = 5.6466\times10^{12}$Pa, $E_{22}^{cn} = 7.08\times10^{12}$Pa, $G_{12}^{cn} = 1.9445\times10^{12}$Pa, $\nu_{12}^{cn} = 0.175$, $\rho_{cn} = 1.4\times10^3$ kg/m^3 at room temperature (T=300 K) are selected as the reinforcements. The CNT/matrix efficiency parameters for volume fraction of CNTs are tabulated in Table 1 [20].

4.2. Examples for validation

Example 1: To check the accuracy of current study, our results for homogeneous isotropic HYPARSSs are compared with the results of Ref. [40] within the couple stress theory (CST). In comparison, the expression (19) is used for the calculation of ω_L . For the non-dimensional frequency parameter $\bar{\omega}_L$, the following formula $\bar{\omega}_L = \omega_L h\sqrt{\rho_m/G_m}$ is used, as in the study of Matsunaga [40]. The material properties are; $E_m = 7\times10^{10}$Pa, $G_m = 0.5E_m/(1+\nu_m)$, $\nu_m = 0.3$ and the geometric data are presented in Table 2.

Table 1. CNT/matrix efficiency parameters for volume fraction of CNTs

V_{cnt}^{*}	η_1	η_2	η_3
0.12	0.137	1.022	0.715
0.17	0.142	1.626	1.138
0.28	0.141	1.585	1.109

Table 2. Comparison the natural frequency of homogeneous HYPARSSs within the CST (a / b = 1)

			$\overline{\omega}_L$	
a / h	a / R_1	b / R_2	Matsunaga [40]	Present study
10	0.2	-0.2	0.09276	0.09432
20	0.2	-0.2	0.02349	0.02408

Table 3. Variation of the natural frequency of HYPARSSs reinforced with different CNT distributions depending on the R_1 / a ratio for different V_{cn}^*.

		UD		FG-V		FG-O		FG-X	
V_{cn}^*	R_1 / a				ω_L				
0.12	1	0.792	0.903	0.695	0.762	0.695	0.762	0.903	1.089
	2	1.585	1.807	1.391	1.523	1.391	1.523	1.805	2.178
	3	2.377	2.710	2.086	2.285	2.086	2.285	2.708	3.266
	4	3.169	3.613	2.781	3.047	2.781	3.047	3.610	4.355
0.17	1	0.972	1.091	0.851	0.920	0.851	0.920	1.111	1.316
	2	1.945	2.181	1.701	1.839	1.701	1.839	2.223	2.631
	3	2.917	3.272	2.552	2.759	2.552	2.759	3.334	3.947
	4	3.890	4.363	3.402	3.679	3.402	3.679	4.446	5.263
0.28	1	1.155	1.354	1.018	1.132	1.018	1.132	1.295	1.646
	2	2.310	2.709	2.036	2.265	2.036	2.265	2.590	3.292
	3	3.465	4.063	3.054	3.397	3.054	3.397	3.886	4.938
	4	4.620	5.417	4.071	4.530	4.071	4.530	5.181	6.584

4.3. Nonlinear vibration of HYPARSSs reinforced by CNTs

The new analyzes on the linear and NLV frequencies of HYPARSSs reinforced with carbon nanotubes distributing as a linear function are performed using Eqs. (19), (24) and (25). The values of frequency of HYPARSSs reinforced with uniformly distributed CNTs are also calculated to determine the influences of CNT distributions as a linear function on the linear and nonlinear frequencies. The geometry of HYPAR shells and other data are presented either on the figures or in comments part.

Table 3 shows the variation of the natural frequency of HYPARSSs reinforced with four different CNT distributions (UD, FG-V, FG-O and FG-X), depending on the R_1 / a ratio for different V_{cn}^*. $a = b, a = 20h$, $(m = 1, n = 1)$. When the CNT changes in a linear function in the direction of the matrix thickness, the influences of the material gradient on the frequency become more pronounced with the increase of V_{cn}^*. In FG-V and FG-O-type distributions, although influence of the heterogeneity is approximately the same (15.6%), as the natural frequencies are compared with the UD-profile, this influence is more pronounced (20.5%) in the FG-X-type distribution of CNTs. Increasing the R_1 / a ratio does not change the heterogeneity effect on the natural frequency.

In Fig. 2, the influence of the distribution of CNTs in the form of a linear function on the frequency of NLV versus f is presented by comparing it with the FG-V- HYPARSS. The HYPARSS characteristics are presented on the Fig. 2. The lowest values of nonlinear frequency are found in the FG-V-type HYPARSS as compared to other types of HYPARSSs. As can be seen, although the nonlinear frequency values of HYPARSSs increase with an increase of f, the influence of the nonuniform CNT distribution on the values of frequency for NLV is significantly weakened. For example, the influence of nonuniform CNT distribution on the nonlinear frequency values for HYPARSS with FG-X-type distribution decreases from 12% to 7.23%, as the f increases from 0.2 to 1.0.

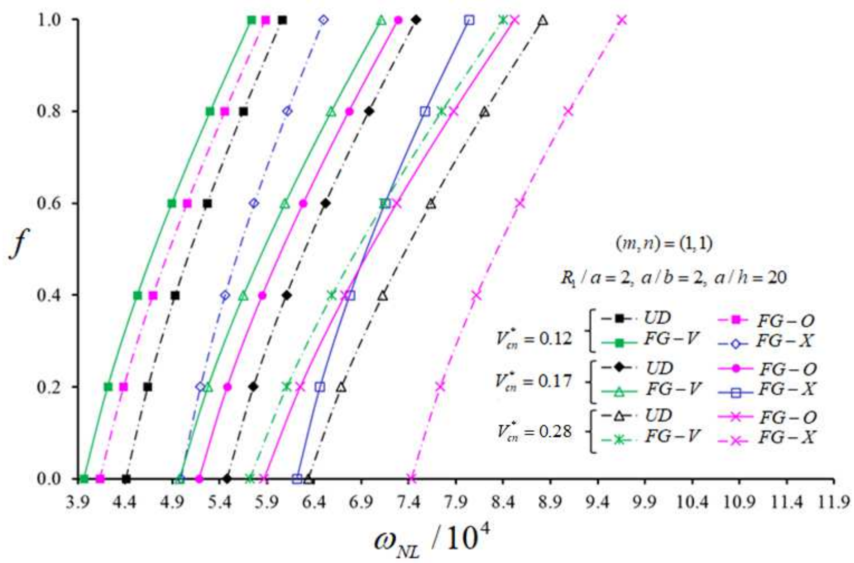

Fig. 2. Variation of the nonlinear frequency of HYPARSSs reinforced with different CNT distributions versus the f for different V_{cn}^*

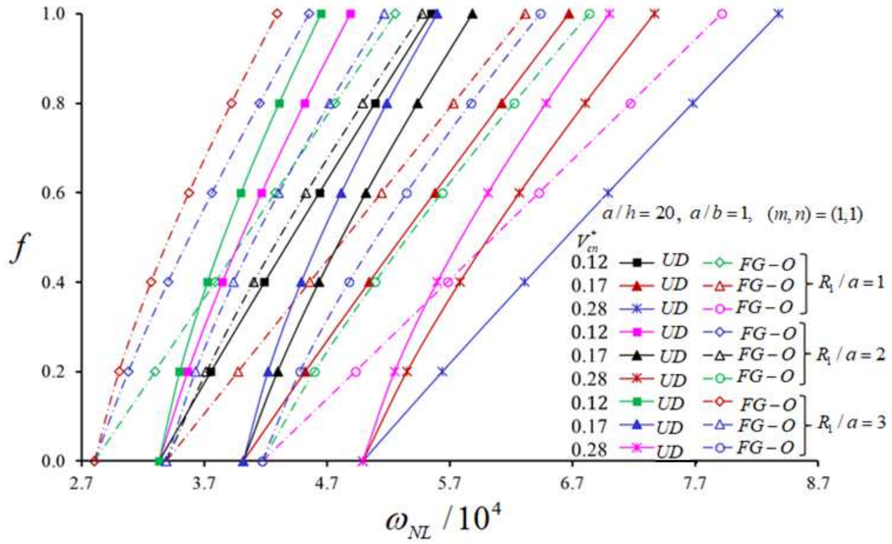

Fig. 3. Variation of the ω_{NL} of HYPARSSs reinforced with different CNT distributions depending on the f for different V_{cn}^* and R_1/a.

The influence of the distribution of CNTs as a linear function of the FG-O-type on the frequency of NLV for HYPARSS, when compared with the UD- HYPARSS, depending on the change of the f, for different R_1/a is presented in Fig. 3. The other characteristics of HYPARSSs are presented on the Fig. 3. It is seen that the nonlinear frequency values of FG-O- HYPARSS are lower than the values of UD-type HYPARSS for all V_{cn}^*. Although the NL frequency values of HYPARSSs decrease with the increase of R_1/a ratio, the heterogeneity effect does not change. Although the frequency values of NLV for FG-O and UD- HYPARSSs increase with the increase of the f, the influence of the FG-O -type heterogeneous distribution of the CNT on the nonlinear frequency values decreases significantly.

The influence of the distribution of CNTs as a linear function of the FG-O-type on the nonlinear frequency of HYPARSS, when compared with the UD- HYPARSS, depending on the change of the f, for different (m,n) modes is presented in Table 4. The HYPARSS parameters are: $a=0.5R_1$, $b=0.5a$, $h=0.05a$. For the (m,n) modes, when the number of waves n increases from 1 to 3, the influence of the distribution of FG-O-type CNTs on the NL frequency of HYPARSS is the smallest at $n=2$, then it increases with increasing n, while the effect is continuous and significantly with increasing of the m waves. Increasing f is reduced the rate of increase of the heterogeneity.

Table 4. Variation of the ω_{NL} of HYPARSSs reinforced with FG-O-type CNT distributions depending on the f for different V_{cn}^*.

		$V_{cn}^*=0.12$		$V_{cn}^*=0.17$		$V_{cn}^*=0.28$	
		UD	FG-O	UD	FG-O	UD	FG-O
(m,n)	f	$\omega_{NL}/10^4$					
(1,1)	0	4.408	4.132	5.482	5.179	6.335	5.869
	0.2	4.639	4.383	5.759	5.477	6.687	6.253
	0.4	4.929	4.694	6.108	5.850	7.125	6.727
	0.6	5.268	5.054	6.519	6.284	7.635	7.272
	0.8	5.648	5.453	6.980	6.767	8.202	7.874
	1	6.060	5.883	7.482	7.290	8.815	8.521
(1,2)	0	10.545	10.637	13.522	13.702	14.434	14.687
	0.2	10.641	10.732	13.644	13.825	14.565	14.823
	0.4	10.923	11.015	14.006	14.188	14.954	15.224
	0.6	11.377	11.470	14.588	14.773	15.579	15.870
	0.8	11.985	12.078	15.367	15.555	16.415	16.732
	1	12.723	12.817	16.313	16.507	17.431	17.779
(1,3)	0	21.480	21.734	27.681	28.123	29.168	29.963
	0.2	21.733	21.988	28.004	28.448	29.517	30.320
	0.4	22.403	22.659	28.866	29.314	30.433	31.262
	0.6	23.455	23.712	30.221	30.675	31.867	32.736
	0.8	24.840	25.098	32.006	32.469	33.752	34.675
	1	26.507	26.765	34.155	34.628	36.019	37.006
(2,1)	0	13.318	11.231	16.081	13.560	19.968	16.697
	0.2	13.460	11.399	16.251	13.761	20.183	16.953
	0.4	13.876	11.887	16.749	14.347	20.813	17.700
	0.6	14.542	12.659	17.549	15.274	21.824	18.880
	0.8	15.428	13.667	18.611	16.484	23.165	20.417
	1	16.496	14.863	19.894	17.920	24.782	22.238
(3,1)	0	29.230	24.363	35.167	29.248	44.046	36.433
	0.2	29.616	24.824	35.630	29.799	44.634	37.137
	0.4	30.616	26.006	36.828	31.218	46.150	38.944
	0.6	32.171	27.819	38.692	33.395	48.508	41.709
	0.8	34.207	30.149	41.133	36.193	51.593	45.258
	1	36.643	32.885	44.054	39.479	55.284	49.422

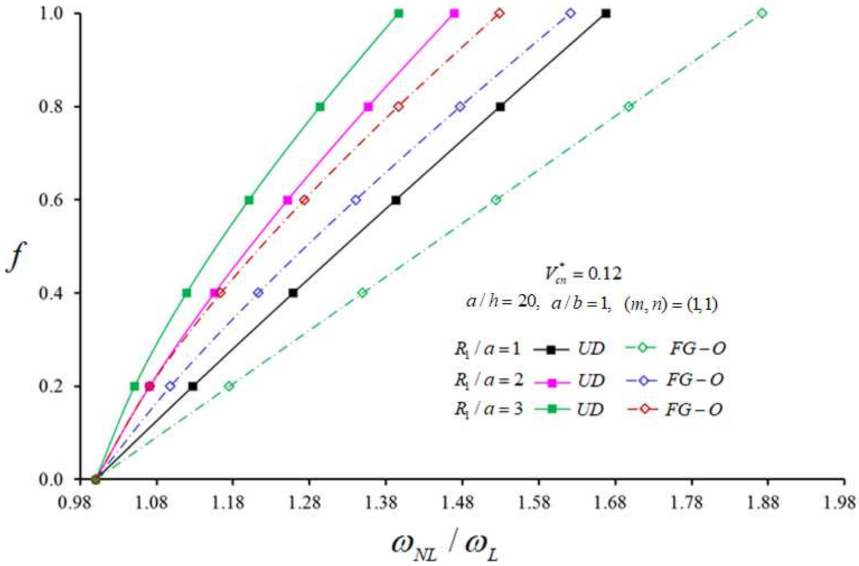

Fig. 4. Variation of the ratio ω_{NL} / ω_L for UD- and FG-O- HYPARSSs versus the f

The change of the ratio ω_{NL} / ω_L for UD- and FG-O- HYPARSSs depending on the f is shown in Fig. 4 for $V_{cn}^* = 0.12$. It is observed that the ω_{NL} / ω_L ratio of the FG-O- HYPARSS is greater than that of the UD- HYPARSS. These ratios increase, and the difference between them becomes wider with increasing f. For example, with f = 0.2 this difference is around 2.5%, while with f = 1.0 it is around 10.3%.

5. Conclusions

The analytical solution of the nonlinear frequency for carbon nanotube-based hyperbolic paraboloidal shallow shells with various distributions is presented. A theoretical model was created for carbon nanotube-based hyperbolic paraboloidal shallow shells using the von Kármán -type nonlinearity. Then the NL partial differential equations are reduced to ordinary NL differential equations using Galerkin methods and the correlation for frequency-amplitude relationship is obtained using Grigolyuk method. In addition, the nonlinear frequency / linear frequency ratio is determined as a function of amplitude. The accuracy of the obtaining formulas is verified by comparison with the results in the literature.

Numerical analysis led to the following generalized results:

a) The nonlinear frequency values of hyperbolic paraboloidal shallow shells increase with an increase of the non-dimensional amplitude, while the influence of the nonuniform carbon nanotube distribution on the values of nonlinear frequency is significantly weakened.
b) In FG-V and FG-O-type distributions, although influence of the FG-profiles is approximately the same, as the natural frequencies are compared with the UD-profile this influence is more pronounced in the FG-X-type distribution of carbon nanotubes.
c) The lowest values of nonlinear frequency are found in the FG-V-type hyperbolic paraboloidal shallow shell as compared to other types of hyperbolic paraboloidal shallow shells.
d) Although the nonlinear frequency values of hyperbolic paraboloidal shallow shells decrease with the increase of R_1 / a ratio, the effect of FG profiles does not change.
e) The nonlinear to linear frequency ratio of the FG-O- hyperbolic paraboloidal shallow shells is greater than that of the UD- hyperbolic paraboloidal shallow shell and the difference between them becomes wider with increasing of the nondimensional amplitude.
f) At the number of waves n increases, the influence of the distribution of FG-O-type carbon nanotubes on the nonlinear frequency is the smallest at $n = 2$, then it increases with increasing of n, while the effect of the FG-O profile is continuous and significantly with increasing of m waves.

Author Contributions

E. Yusufoglu planned the Formal analysis, Investigation, Validation, Writing—Original Draft and Writing—Review & Editing; M. Avey conducted Investigation, Validation, Writing—Original Draft and Writing—Review & Editing. The manuscript was written through the contribution of all authors. All authors discussed the results, reviewed, and approved the final version of the manuscript.

Conflict of Interest

The authors declared no potential conflicts of interest with respect to the research, authorship, and publication of this article.

Funding

The authors received no financial support for the research, authorship, and publication of this article.

References

[1] Candela, F., Structural applications of hyperbolic paraboloidal shells. *Journal of the American Concrete Institute,* 26(5), 1955, 397-415.
[2] Chen, J.F., Buckling of composite hyperbolic paraboloidal shells. *Journal of Building Structures*, 13(4), 1992, 28-34.

[3] Chakravorty, D., Bandyopadhyay, J.N., On the free vibration of shallow shells. *Journal of Sound and Vibration*, 185(4), 1995, 673–684.
[4] Liew, K.M., Lim, C.W., Kitipornchai, S. Vibration of shallow shells: a review with bibliography. *Applied Mechanics Reviews*, 50, 1997, 431–444.
[5] Sahoo, S., Chakravorty, D., Finite element vibration characteristics of composite hypar shallow shells with various edge supports. *Journal Vibration and Control*, 11(10), 2005, 1291-1309.
[6] Tornabene, F., Viola, E., 2-D solution for free vibrations of parabolic shells using generalized differential quadrature method. *European Journal of Mechanics A/Solids*, 27(6), 2008, 1001–1025.
[7] Jiang, S., Yang, T., Li, W.L., Du, J., Vibration analysis of doubly curved shallow shells with elastic edge restraints. *Journal of Vibration and Acoustics*, 135(3), 2013, 034502.
[8] Tornabene, F., Fantuzzi, N., Bacciocchi, M., Neves, A.M.A., Ferreira, A.J.M., MLSDQ based on RBFs for the free vibrations of laminated composite doubly-curved shells. *Composites Part B-Engineering*, 99, 2016, 30-47.
[9] Pang, F., Li, H., Wang, X., Miao, X., Li, S., A semi analytical method for the free vibration of doubly-curved shells of revolution. *Computers & Mathematics with Applications*, 75(9), 2018, 3249-3268.
[10] Brischetto, S., Tornabene, F., Advanced GDQ models and 3D stress recovery in multilayered plates, spherical and double-curved panels subjected to transverse shear loads. *Composites Part B-Engineering*, 146, 2018, 244-269.
[11] Iijima, S., Helical microtubules of graphitic carbon. *Nature,* 354, 1991, 56–58.
[12] Ajayan, P.M., Stephan, O., Colliex, C., Trauth, D. Aligned carbon nanotube arrays formed by cutting a polymer resin-nanotube composite. *Science*, 265, 1994, 1212-1214.
[13] Falvo, MR; Clary, G.J., Taylor, RM., Chi, V., Brooks, F.P., Washburn, S., Superfine, R., Bending and buckling of carbon nanotubes under large strain. *Nature*, 389(6651), 1997, 582-584.
[14] Ajayan, P.M., Tour, J.M., Materials science - Nanotube composites. *Nature,* 447(7148), 2007, 1066-1068.
[15] Lau, K.T., Hui, D., The revolutionary creation of new advanced materials – carbon nanotube composites. *Composites Part B-Engineering*, 33, 2002, 263–277.
[16] Shaffer, M., Kinloch, I.A., Prospects for nanotubes and nanofiber composites. *Composites Science and Technology*, 64, 2004, 2281–2282.
[17] Silvestre, J., Silvestre, N., De Brito, J., Polymer nanocomposites for structural applications: Recent trends and new perspectives. *Mechanics of Advanced Materials and Structures*, 23(11), 2016, 1263-1277.
[18] Hu, N., Fukunaga, H., Lu, C., Kameyama, M., Yan, B., Prediction of elastic properties of carbon nanotube reinforced composites. *Proceedings of the Royal Society A,* 461, 2005, 1685–1710.
[19] Roy, N., Sengupta, R., Bhowmick, A.K., Modifications of carbon for polymer composites and nanocomposites. *Progress in Polymer Sciences*, 37, 2012, 781–819.
[20] Shen, H.S., Nonlinear bending of functionally graded carbon nanotube-reinforced composite plates in thermal environments. *Composite Structures*, 91(1), 2009, 9–19.
[21] Shen, H.S, He, X.Q. Large amplitude free vibration of nanotube-reinforced composite doubly curved panels resting on elastic foundations in thermal environments. *Journal of Vibration and Acoustics*, 23(16), 2017, 2672–2689.
[22] Duc, N.D., Quan, T.Q., Khoa, N.D., New approach to investigate nonlinear dynamic response and vibration of imperfect functionally graded carbon nanotube reinforced composite double curved shallow shells subjected to blast load and temperature. *Aerospace Science and Technology*, 71, 2017, 360-372.
[23] Sheng, G.G, Wang, X., The non-linear vibrations of rotating functionally graded cylindrical shells. *Nonlinear Dynamics*, 87, 2017, 1095–1109.
[24] Li, H., Pang, F., Gong, Q., Teng, Y., Free vibration analysis of axisymmetric functionally graded doubly curved shells with un-uniform thickness distribution based on Ritz method. *Composite Structures*, 225, 2019, 111145.
[25] Amir, M., Talha, M., Nonlinear vibration characteristics of shear deformable functionally graded curved panels with porosity including temperature effects. *International Journal of Pressure Vessels and Piping*, 172, 2019, 28-41.
[26] Zghal, S., Frikha, A., Dammak, F., Large deflection responses-based geometrical nonlinearity of nanocomposite structures reinforced with carbon nanotubes. *Applied Mathematics and Mechanics (English Edition)*, 41, 2020, 1227–1250.
[27] Sofiyev, A.H., Turan, F., Zerin, Z., Large-amplitude vibration of functionally graded orthotropic double-curved shallow spherical and hyperbolic paraboloidal shells, *International Journal of Pressure Vessels and Piping,* 188, 2020, 104235.
[28] Duc, N.D., Nam, V.H., Cuong, N.H., Nonlinear postbuckling of eccentrically oblique-stiffened functionally graded doubly curved shallow shells based on improved Donnell equations. *Mechanics of Composite Materials*, 55(6), 2020, 727-742.
[29] Jena, S.K., Chakraverty, S., Malikan, M., Application of shifted Chebyshev polynomial-based Rayleigh–Ritz method and Navier's technique for vibration analysis of a functionally graded porous beam embedded in Kerr foundation. *Engineering with Computers*, 2020, 1-21, https://doi.org/10.1007/s00366-020-01018-7.
[30] Jena, S.K., Chakraverty, S., Malikan, M., Sedighi H.M., Implementation of Hermite–Ritz method and Navier's technique for vibration of functionally graded porous nanobeam embedded in Winkler–Pasternak elastic foundation using bi-Helmholtz nonlocal elasticity. *Journal of Mechanics of Materials and Structures*, 15(3), 2020, 405-434.
[31] Jena, S.K., Chakraverty, S., Malikan, M., Tornabene, F., Stability analysis of single-walled carbon nanotubes embedded in Winkler foundation placed in a thermal environment considering the surface effect using a new refined beam theory. *Mechanics Based Design of Structures and Machines*, 2020, 1-15, https://doi.org/10.1080/15397734.2019.1698437.
[32] Avey, M., Yusufoglu, E., On the solution of large-amplitude vibration of carbon nanotube-based doubly-curved shallow shells. *Mathematical Methods in the Applied Sciences*, 2020, 1-10, https://doi.org/10.1002/mma.6820.
[33] Malikan, M., Eremeyev, V.A., On the geometrically nonlinear vibration of a piezo-flexomagnetic nanotube. *Mathematical Methods in the Applied Sciences*, 2020, 1-12, https://doi.org/10.1002/mma.6758.
[34] Malikan, M., Eremeyev, V.A., Sedighi H.M., Buckling analysis of a non-concentric double-walled carbon nanotube. *Acta Mechanica*, 231, 2020, 5007–5020.
[35] Malikan, M., Uglov NS, Eremeyev, V.A., On instabilities and post-buckling of piezomagnetic and flexomagnetic nanostructures. *International Journal of Engineering Science*, 157, 2020, 103395.
[36] Malikan, M., Eremeyev, V.A., A new hyperbolic-polynomial higher-order elasticity theory for mechanics of thick FGM beams with imperfection in the material composition. *Composite Structures*, 249, 2020, 112486.
[37] Malikan, M., Nguyen, V.B., Tornabene, F., Dimitri, R., Dynamic modeling of non-cylindrical curved viscoelastic single-walled carbon nanotubes based on the second gradient theory. *Materials Research Express*, 6, 2019, 075041.
[38] Volmir, A.S., *The nonlinear dynamics of plates and shells*, Science Edition, Moscow, 1972.
[39] Grigolyuk, E.I., On vibrations of a shallow circular cylindrical panel experiencing finite deflections. *Applied Mathematics and Mechanics*, 19(3), 1955, 386-382.
[40] Matsunaga, H., Vibration and stability of thick simply supported shallow shells subjected to in-plane stresses. *Journal of Sound and Vibration*, 225(1), 1999, 41–60.

ORCID iD

Elçin Yusufoglu https://orcid.org/0000-0001-8091-5785
Mahmure Avey https://orcid.org/0000-0002-9963-0955

How to cite this article: Yusufoglu E., Avey M. Nonlinear Dynamic Behavior of Hyperbolic Paraboloidal Shells Reinforced by Carbon Nanotubes with Various Distributions, *J. Appl. Comput. Mech.*, 7(2), 2021, 913–921. https://doi.org/10.22055/JACM.2021.36043.2783